Poly(ADP-ribose)polymerases are involved in micro-homology mediated back-up non-homologous end-joining in Arabidopsis thaliana

Jia, Q.; Dulk, H. den; Shen, H.; Hooykaas, P.J.J.; Pater, S. de

Plant Mol Biol (2013) 82:339–351
DOI 10.1007/s11103-013-0065-9

Poly(ADP-ribose)polymerases are involved in microhomology mediated back-up non-homologous end joining in *Arabidopsis thaliana*

Qi Jia · Amke den Dulk-Ras · Hexi Shen · Paul J. J. Hooykaas · Sylvia de Pater

Received: 15 January 2013 / Accepted: 20 April 2013 / Published online: 28 April 2013

Abstract Besides the KU-dependent classical non-homologous end-joining (C-NHEJ) pathway, an alternative NHEJ pathway first identified in mammalian systems, which is often called the back-up NHEJ (B-NHEJ) pathway, was also found in plants. In mammalian systems PARP was found to be one of the essential components in B-NHEJ. Here we investigated whether PARP1 and PARP2 were also involved in B-NHEJ in Arabidopsis. To this end Arabidopsis *parp1*, *parp2* and *parp1parp2* (*p1p2*) mutants were isolated and functionally characterized. The *p1p2* double mutant was crossed with the C-NHEJ *ku80* mutant resulting in the *parp1parp2ku80* (*p1p2k80*) triple mutant. As expected, because of their role in single strand break repair (SSBR) and base excision repair (BER), the *p1p2* and *p1p2k80* mutants were shown to be sensitive to treatment with the DNA damaging agent MMS. End-joining assays in cell-free leaf protein extracts of the different mutants using linear DNA substrates with different ends reflecting a variety of double strand breaks were performed. The results showed that compatible 5′-overhangs were accurately joined in all mutants, that KU80 protected the ends preventing the formation of large deletions and that PARP proteins were involved in microhomology mediated end joining (MMEJ), one of the characteristics of B-NHEJ.

Keywords Arabidopsis · Back-up NHEJ · Comet assay · End joining · PARP

Introduction

For living organisms, DNA double strand breaks (DSBs) are one of the most harmful lesions that can promote mutation and induce cell death. To maintain genetic stability, organisms have developed two main pathways for DNA repair of DSBs (Hiom 2010). One is the homologous recombination (HR) pathway involving extensive DNA sequence homology between the interacting molecules (San Filippo et al. 2008), and the other is the non-homologous end-joining (NHEJ) pathway acting independently of significant homology (Lieber 2010). HR occurs during the late S to G2 phases of the cell cycle when the sister chromatid is in close proximity as repair template. On the other hand, NHEJ does not require a homologous chromosome and can function throughout the cell cycle. NHEJ is more error-prone than HR and often produces short deletions and insertions. Emerging evidence suggests that the relative balance of the two pathways is tuned to minimize the mutagenesis as a consequence of repair (Shrivastav et al. 2008).

Distinct NHEJ pathways have been identified in mammals (Mladenov and Iliakis 2011). One is the classical NHEJ (C-NHEJ) pathway, which is dependent on KU70/KU80 and DNA-PKcs. DNA ligase IV (LIG4), XRCC4 and XLF/Cernunnos are also utilized as central components in

Electronic supplementary material The online version of this article (doi:10.1007/s11103-013-0065-9) contains supplementary material, which is available to authorized users.

Q. Jia · A. d. Dulk-Ras · H. Shen · P. J. J. Hooykaas · S. de Pater (✉)
Department of Molecular and Developmental Genetics, Institute of Biology, Leiden University, Sylviusweg 72, 2333 BE Leiden, The Netherlands
e-mail: b.s.de.pater@biology.leidenuniv.nl

Present Address:
Q. Jia
College of Crop Science, Fujian Agriculture and Forestry University, Fuzhou, China

C-NHEJ. In the absence of C-NHEJ core factors, back-up NHEJ (B-NHEJ) pathways become active, which accounts for residual end joining of DSBs (Nussenzweig and Nussenzweig 2007; Haber 2008; Iliakis 2009). Some proteins have been shown to be involved in B-NHEJ, such as poly(ADP-ribose)polymerase 1 (PARP1), PARP2, DNA ligase III (LIG3) and X-ray repair cross-complementing group 1 (XRCC1) (Wang et al. 2003; Audebert et al. 2004). XRCC1 was initially found to be involved in repair of DNA single-strand breaks (Caldecott 2003). It interacts with PARP1 and PARP2, which is stimulated by DNA damage. XRCC1 also interacts with LIG3, preventing degradation of LIG3 by the proteasome (Caldecott 2003). More recently, also histone H1 (Rosidi et al. 2008), XPF (Ahmad et al. 2008) and MRE11 (Xie et al. 2009; Cheng et al. 2011) were found to play a role in B-NHEJ. In the absence of C-NHEJ, microhomologous sequences (5–25 bps), flanking the break, are more frequently used to join the DNA ends, resulting in deletions (Kuhfittig-Kulle et al. 2007). This error-prone pathway has been called microhomology mediated end joining (MMEJ) (McVey and Lee 2008). It seemed that MMEJ is the predominant pathway among the B-NHEJ pathways. The kinetics of DNA repair via B-NHEJ appears to be slower than C-NHEJ (Dibiase et al. 2000; Wang et al. 2006) and is enhanced in G2 (Wu et al. 2008). When KU is absent, PARP and MRE11 are mobilized to damaged chromatin (Cheng et al. 2011).

In plants, orthologs of the C-NHEJ components KU70, KU80, LIG4 and XRCC4 (West et al. 2000, 2002; Tamura et al. 2002; Riha et al. 2002; Bundock et al. 2002) have been identified. *Agrobacterium tumefaciens* T-DNA integration, which occurs mainly via NHEJ, still occurred in the *lig4, ku70* and *ku80* NHEJ mutants (Friesner and Britt 2003; van Attikum et al. 2003; Gallego et al. 2003; Li et al. 2005; Jia et al. 2012), although a lower transformation frequency was reported in several cases (Friesner and Britt 2003; Li et al. 2005; Jia et al. 2012). This observation has led to the postulation of alternative NHEJ pathways in plants as well. Further research showed that end joining still occurred in a *ku70* mutant, since the frequency of chromosome fusions was not decreased (Puizina et al. 2004; Heacock et al. 2004) and that plasmid end joining in *ku80* protoplasts was still observed although at a lower frequency (Gallego et al. 2003). Orthologs of XRCC1 and XPF have also been identified in Arabidopsis and T-DNA insertion mutants have been characterized (Fidantsef et al. 2000; Uchiyama et al. 2008). Using single and double mutants, it was shown that slow repair of γ radiation-induced DSBs in the *ku80* mutant was dependent on XRCC1 (Charbonnel et al. 2010) and XPF (Charbonnel et al. 2011), indicating that these proteins are involved in alternative NHEJ pathways in Arabidopsis. Furthermore MRE11 has been implicated in MMEJ in Arabidopsis, since repair via microhomology was no longer favored after mutation of *MRE11* in a *ku70tert* background (Heacock et al. 2004).

PARPs are ADP-ribose transferases that transfer ADP-ribose (PAR) from NAD^+ to target proteins (Woodhouse and Dianov 2008). Eighteen proteins with the conserved catalytic domain were identified by in silico homology searching in animals (Amé et al. 2004). PARP proteins have a major impact on various cellular processes, such as cell death, transcription, cell division, DNA repair and telomere integrity (Schreiber et al. 2006; Yélamos et al. 2008). Only two of them are activated in response to DNA damage: PARP1 (113 kDa) and PARP2 (62 kDa) (Woodhouse and Dianov 2008). PARP1 is involved in DNA single strand break repair (SSBR) and base excision repair (BER), preventing the formation of DNA double strand breaks (DSBs) (Schreiber et al. 2002; Woodhouse et al. 2008; Masaoka et al. 2009). PARP is thought to detect disrupted replication forks and to attract MRE11 for end processing (Bryant et al. 2009). Recently, PARP3 was also found to be involved in cellular responses to DNA damage (Boehler et al. 2011).

Orthologs of PARP1 and PARP2 have been identified in plants (Babiychuk et al. 1998). One is the classical zinc finger containing polymerase (ZAP), which was first purified from maize seedlings and has a molecular mass of 113 kDa (Chen et al. 1994). It was also identified in Arabidopsis. ZAP has high similarity in the sequence and domain organization to PARP1 in animals. The other one is a structurally non-classical PARP protein, called APP in Arabidopsis and NAP in *Zea mays* (Lepiniec et al. 1995). It is a short version of PARP with the molecular mass of 72 kDa. The counterpart of it in animals has also been identified and was termed PARP2 (Amé et al. 1999). Since APP was identified earlier than ZAP in Arabidopsis, APP is sometimes referred to as PARP1 and ZAP as PARP2 (De Block et al. 2005). Considering the similarity to the corresponding homologs in animals and according to the nomenclature used at The Arabidopsis Information Resource (TAIR) website (www.arabidopsis.org), in this paper ZAP was termed PARP1 (At2g31320) and APP was termed PARP2 (At4g02390). Former reports on PARP1 and PARP2 in plants provide evidence for the function of PARP in stress tolerance and in the control of programmed cell death (Amor et al. 1998; De Block et al. 2005; Vanderauwera et al. 2007).

In order to investigate whether the PARP orthologs in plants are involved in the back-up NHEJ pathway, *parp1* and *parp2* T-DNA insertion mutants were functionally characterized along with the *parp1parp2* (*p1p2*), *ku80* and *parp1parp2ku80* (*p1p2k80*) mutants for the sensitivity to DNA damaging agents and the capacity for in vitro DNA end joining of linear DNA substrates with different ends.

Materials and methods

Plant material

The *parp1* (At2g31320) T-DNA insertion line was obtained from the GABI-Kat T-DNA collection (GABI-Kat Line 692A05) (Li et al. 2007). The *parp2* (At4g02390) T-DNA insertion line was obtained from the SALK T-DNA collection (SALK_640400) (Alonso et al. 2003). The *ku80* (At1g48050) T-DNA insertion line (SALK_016627) was described previously (Jia et al. 2012).

Molecular analysis of the plant lines

The T-DNA insertion sites were mapped with a T-DNA Left Border (LB) specific primer (LBa1 for the SALK line and SP173 for the GABI-Kat line) or a T-DNA Right border (RB) specific primer (SP200 for the GABI-Kat line) and a gene-specific primer and the PCR products were sequenced. Pairs of gene-specific primers around the insertion site were used to determine whether the plants were homozygous or heterozygous for the T-DNA insertion. The sequences of all the primers are listed in Table S1. For Southern blot analysis, DNA was extracted using a CTAB DNA isolation protocol (de Pater et al. 2006) and digested with *Eco*RV or *Bg*lII (*parp1*) or *Hin*dIII (*parp2*). DNA (5 µg) was ran on a 0.7 % agarose gel and transferred onto positively charged Hybond-N membrane (Amersham Biosciences). The hybridization and detection procedures were done according to the DIG protocol from Roche Applied Sciences. The DIG probe was produced using the PCR DIG Labeling Mix (Roche) with specific primers SP225 and SP226 that amplified a fragment of the T-DNA of pGABI1 (*parp1*) or specific primers SP271 and SP272 that amplified a fragment from the T-DNA of pROK2 (*parp2*).

Quantitative reverse-transcription PCR (Q-RT-PCR)

Leaves of 2-week-old plants were ground under liquid N_2 in a Tissue-Lyser (Retch). Total RNA was extracted from the leaf powder using the RNeasy kit (Qiagen) according to the supplied protocol. Residual DNA was removed from the RNA samples with DNaseI (Ambion) in the presence of RNase inhibitor (Promega). RNA was quantified and was used to make cDNA templates using an iScript cDNA synthesis kit according to the manufacturer's instructions (Bio-Rad). Quantitative real-time PCR (Q-PCR) analyses were done using the iQ™ SYBR® Green Supermix (Bio-Rad). Specific fragments (about 200 bp) were amplified by pairs of primers around the T-DNA insertion sites using a DNA Engine Thermal Cycler (MJ Research) equipped with a Chromo4 real-time PCR detection system (Bio-Rad). The sequences of the primers are listed in Table S1. The cycling parameters were 95 °C for 3 min, 40 cycles of (95 °C for 1 min, 60 °C for 40 s), 72 °C for 10 min. All sample values were normalized to the values of the house keeping gene *ROC1* (At4g38740) (primers ROC5.2, ROC3.3) and were presented as relative expression ratios. The value of the wild type was set on 1.

Assays for sensitivity to methyl methane sulfonate (MMS)

Seeds of wild type, *parp1*, *parp2*, *p1p2*, *ku80* and *p1p2k80* were germinated on solid ½ MS medium without additions or on ½ MS medium containing MMS (Sigma). For assays in liquid medium, 4-days-old seedling were transferred to liquid ½ MS medium without additions or ½ MS medium containing MMS (Sigma). The seedlings were scored after 2 weeks of growth. Fresh weight (compared with controls) was determined by weighing the seedlings in batches of 20 in triplicate, which were treated in liquid ½ MS with MMS for 2 weeks. In order to obtain normally distributed residuals, log values of fresh weight were used for analysis. One-Way ANOVA tests with pair wise comparison of means were performed to test for significant differences ($P < 0.05$) between plant lines for each treatment (software "R Through Excel"). For each test residuals (difference between mean and observed values) were checked for equal distribution over the whole range and for normal distribution with Shapiro–Wilk Normality tests.

Comet assay

One-week-old seedlings were treated in liquid ½ MS containing 0.01 % MMS for 0 h, 2 h, 24 h or 24 h followed by 24 h recovery in liquid ½ MS. DNA damage was detected by comet assays as described previously (Menke et al. 2001) with minor modifications. DNA was exposed to high alkali prior to electrophoresis under neutral conditions (A/N protocol) to detect DNA SSBs as well as DSBs. Plant nuclei were embedded in 1 % low melting point Ultrapure™ agarose-1000 (Invitrogen) to make a mini gel on microscopic slides according to the protocol. Nuclei were lysed in high alkali (0.3 M NaOH, 5 mM EDTA pH13.5) for 20 min at room temperature. Equilibration for 3 times 5 min in TBE buffer (90 mM Tris–borate, 2 mM EDTA, pH8.4) on ice was followed by electrophoresis at 4 °C (cold room) in TBE buffer for 15 min at 30 V (1 V/cm), 15–17 mA. Dry agarose gels were stained with 15 µl ethidium bromide (5 µg/ml) and immediately evaluated with a Zeiss Axioplan 2 imaging fluorescence microscope (Zeiss, Germany) using the DsRed channel (excitation at 510 nm, emission at 595 nm). Images of comets were captured at a 40-fold magnification by an AxioCam MRc5 digital camera (Zeiss,

Germany). The comet analysis was carried out by comet scoring software CometScore™ (Tritek Corporation). The fraction of DNA in comet tails (%tail-DNA) was used as a measure of DNA damage. Measures included 4 independent gel replicas totaling about 100 comets analyzed per experimental point. The results were presented by the mean value ± standard deviation (S.D.) from four gels, based on the median values of %tail-DNA of 25 individual comets per gel. One-Way ANOVA tests with pair wise comparison of means were performed to test for significant differences ($P < 0.05$ or $P < 0.1$) between plant lines for each treatment and between treatments for each plant line (software "R Through Excel"). For each test residuals (difference between mean and observed values) were checked for equal distribution over the whole range and for normal distribution with Shapiro–Wilk Normality tests.

In vitro end-joining assay with protein extract from leaves

Leaves of ten-day-old seedlings were ground under liquid N2 in a Tissue-Lyser (Retch). One ml protein extraction buffer (50 mM Tris–HCl pH 7.5; 2 mM EDTA; 0.2 mM PMSF; 1 mM DTT; 1 × Protease inhibitor cocktail Complete®, EDTA free) was added to 1 g of tissue powder. Soluble protein was isolated by centrifugation at 4 °C. The protein concentration was determined using Bio-Rad protein assay reagent. Glycerol was added to 20 % and the extracts were stored at −80 °C.

The plasmid (pUC18P1/4) (Liang et al. 2008) was amplified using different primer sets (Table S1) to create end-joining substrates. Phusion™ DNA high-fidelity polymerase (Finnzymes) was used for PCR to generate blunt ends (with or without microhomology). Sticky ends were generated by digesting the PCR products with different restriction enzymes. The different ends are listed in Table 1.

The linear DNA substrates (300 ng) were incubated with 1 µg protein extract in 50 mM Tris–HCl (pH 7.6), 10 mM $MgCl_2$, 1 mM DTT, 1 mM ATP and 25 % (w/v) polyethylene glycol 2000 at 14 °C for 2 h in a volume of 20 µl. DNA products were deproteinized and purified by electrophoresis through 0.6 % agarose gels. As negative control linear DNA substrates were incubated without protein extract. A 600 bp fragment containing the end-joined junction was amplified by PCR with q30 and q31 primers flanking the junction and cloned in pJet1.2/blunt (Fermentas). Individual clones were digested by corresponding restriction enzymes to check if they were joined precisely or via MMEJ. The clones resistant to the digestion were sequenced by ServiceXS. When end joining had occurred via MMEJ using the 10 bp microhomology, an *Xcm*I site (CCAN9TGG) was generated. PCR products were digested by *Xcm*I, followed by electrophoresis on a 1.5 % agarose gel. The presence of an *Xcm*I site will result in a 400 and a 200 bp fragment. The intensity of DNA bands was quantified by using ImageJ software. The relative contribution of end joining via the 10 bp repeat was calculated as the percentage of the *Xcm*I-digested fragments of total PCR products (sum of the *Xcm*I- digested and undigested fragments). Chi square tests were used to show significant differences (see Table 2).

Results

Isolation and characterization of T-DNA insertion mutants

End joining still occurred in animal and plant mutants, in which KU70 or KU80 had been inactivated. In animals PARP proteins have been implicated in this KU-independent back-up pathway. In order to find out whether PARP1 and PARP2 play a role in back-up NHEJ (B-NHEJ) in plants, homozygous T-DNA insertion mutants *parp1* and *parp2* were isolated and characterized (Fig. 1). Using T-DNA-specific primers from the left or right border in combination with gene-specific primers flanking the insertion site heterozygous and homozygous mutants were identified. No PCR products were obtained for homozygous mutants using two gene-specific primers. The insertion point of the T-DNA was mapped by sequencing of the PCR products. PCR products were obtained from the LB and RB areas of the *parp1* mutant. The T-DNA of *parp1* turned out to be integrated in exon 14 and had 240 bp filler DNA at the RB end (Fig. 1a). PCR products were obtained with the LB primer combined with gene-specific primers at both sides of the T-DNA insertion for the *parp2* mutant,

Table 1 Substrates with different ends used for end-joining assays

Left end	Right end	Primers
5′ overhang *Bam*HI (G/GATCC)	5′ overhang *Bam*HI (G/GATCC)	q47 + q50
3′ overhang *Kpn*I (GGTAC/C)	3′ overhang *Kpn*I (GGTAC/C)	q48 + q51
3′ overhang *Kpn*I (GGATC/C)	5′ overhang *Eco*RI (G/AATTC)	q48 + q51
Blunt (10 bp repeat)	Blunt (10 bp repeat)	q40 + q41
Blunt	Blunt	q40 + q46

Table 2 Products of in vitro end-joining reactions with linear substrates with different ends

	WT	*p1p2*	*p1p2k80*	*ku80*
*Bam*HI/*Bam*HI	15	17	19	14
Joined precisely (*Bam*HI)	13	17	19	14
Small deletion	2			
*Kpn*I/*Kpn*I	9	12	11	13
Joined precisely (*Kpn*I)	6	7	7	7
Small deletion	2	1	2	1
Large deletion[a]	1			2
Insertion		3	2	3
Substitution		1		
MMEJ (large deletion)[a]				1
*Kpn*I/*Eco*RI	16	12	17	15
Filled-in	5	5	2	3
Small deletion	11	6	13	9
Large deletion[a]		1	2	3
Blunt (no homology)	15	16	11	19
Joined precisely (*Xcm*I)	8	4	1	7
Small deletion	5	11	7	9
Large deletion[a]	2	1	3	3
MMEJ (large deletion)[a]				3
Blunt (10 bp homology)	36	23	17	20
Joined precisely	7	7	3	2
Small deletion	5	10	7	3
Insertion		3	2	
MMEJ (*Xcm*I)[b]	24	3	5	15

Protein extracts of wild-type plants or the *p1p2*, *p1p2k80*, *ku80* mutants were incubated with linear DNA substrates with 5′-overhangs (*Bam*HI), 3′-overhangs (*Kpn*I), incompatible ends (*Kpn*I/*Eco*RI), blunt ends without homology or blunt ends with 10 bp homology. The number of total analyzed products per protein extract (grey rows) and the number of products specified per joining type are shown (small deletion: <10 bp; large deletion: >10 bp). The junctions that were not sensitive for the indicated restriction enzymes were sequenced (Table 3). Significantly more large deletions[a] were obtained with the *ku80* and *p1p2k80* mutants compared to the wild type and the *p1p2* mutant and less MMEJ products[b] were obtained with the *p1p2* and *p1p2k80* mutants compared to the wild type and the *ku80* mutant (Chi square tests)

indicating that at least 2 T-DNA copies had been inserted as an inverted repeat in this locus. The T-DNAs of *parp2* were integrated in intron 6, having 5 bps filler DNA (Fig. 1a).

The genomic DNA was digested by *Eco*RV or *Bgl*II (*parp1*) or *Hin*dIII (*parp2*) for Southern blotting (Fig. 1b). Bands with the expected sizes of 1,350 bp (*Eco*RV), and 2,716 bp (*Bgl*II) were detected for the *parp1* mutant. In the *parp2* mutant, one of expected bands (3,600 bp) from the inverted T-DNAs was detected, but the other expected band (5,476 bp) was not visible, probably because this T-DNA copy is not intact and is missing the *Hin*dIII site. Extra bands were detected, indicating that additional T-DNAs were randomly integrated at other loci.

In order to confirm that the mutants were homozygous indeed and that no mRNA was produced, Q-RT-PCR analysis was performed for the T-DNA insertion lines using primers flanking the insertion site. This resulted in a product for each gene in the wild type, but not in the corresponding T-DNA insertion mutant (results not shown), showing that the mutants were truly homozygous.

The single mutants were crossed and in the next generations, *parp1parp2* (*p1p2*) and *parp1parp2ku80* (*p1p2k80*) homozygous mutants were obtained. No obvious phenotypes were observed in these mutants under standard growth conditions (Fig. 2a).

DNA damage response

In order to determine the sensitivity to DNA-damaging agents single and double mutants were treated with the DNA-damaging agent MMS (Fig. 2a). MMS is a monofunctional alkylating agent that induces *N*-alkyl lesions and SSBs that can be converted into DSBs during replication (O'Connor 1981). Root growth of seedlings of the *parp1* and *parp2* mutants was not significantly more affected by MMS than those of the wild type, whereas the *p1p2* mutant was more sensitive to MMS, with a root length about half the length of the wild type. This indicated redundancy of PARP1 and PARP2 in protection against DNA damage by MMS of the roots. Growth of the *p1p2k80* triple mutant was even further reduced on MMS, indicating that different repair pathways were impaired (Fig. 2a).

To quantify the effect of MMS treatment on growth of the *parp1*, *parp2, p1p2*, *ku80* and *p1p2k80* mutants, the fresh weight of seedlings was determined after 2 weeks of continuous MMS treatment in liquid MS (Fig. 2b). There was no significant difference between the wild type and the *ku80*, *parp1* and *parp2* mutants when grown in the presence of MMS. Previously, a *ku70* mutant was also found to be insensitive to MMS in a similar test (Riha et al. 2002), whereas two other *ku70* mutants (Bundock et al. 2002; Jia et al. 2012) as well as another *ku80* mutant (Gallego et al. 2003) were found to be sensitive to MMS. The difference in sensitivity of the two *ku80* mutants may have been caused by the different ecotypes (Col-0 versus ws) or slightly different experimental conditions. The fresh weight of the *p1p2* mutant was about 50 % of that of the wild type after growth in the presence of 0.008 % MMS, again suggesting partial redundancy of PARP1 and PARP2. The fresh weight of the *p1p2k80* mutant was 25 % of that of the wild type and was significantly different from that of the *p1p2* mutant and the *ku80* mutant. This indicated that

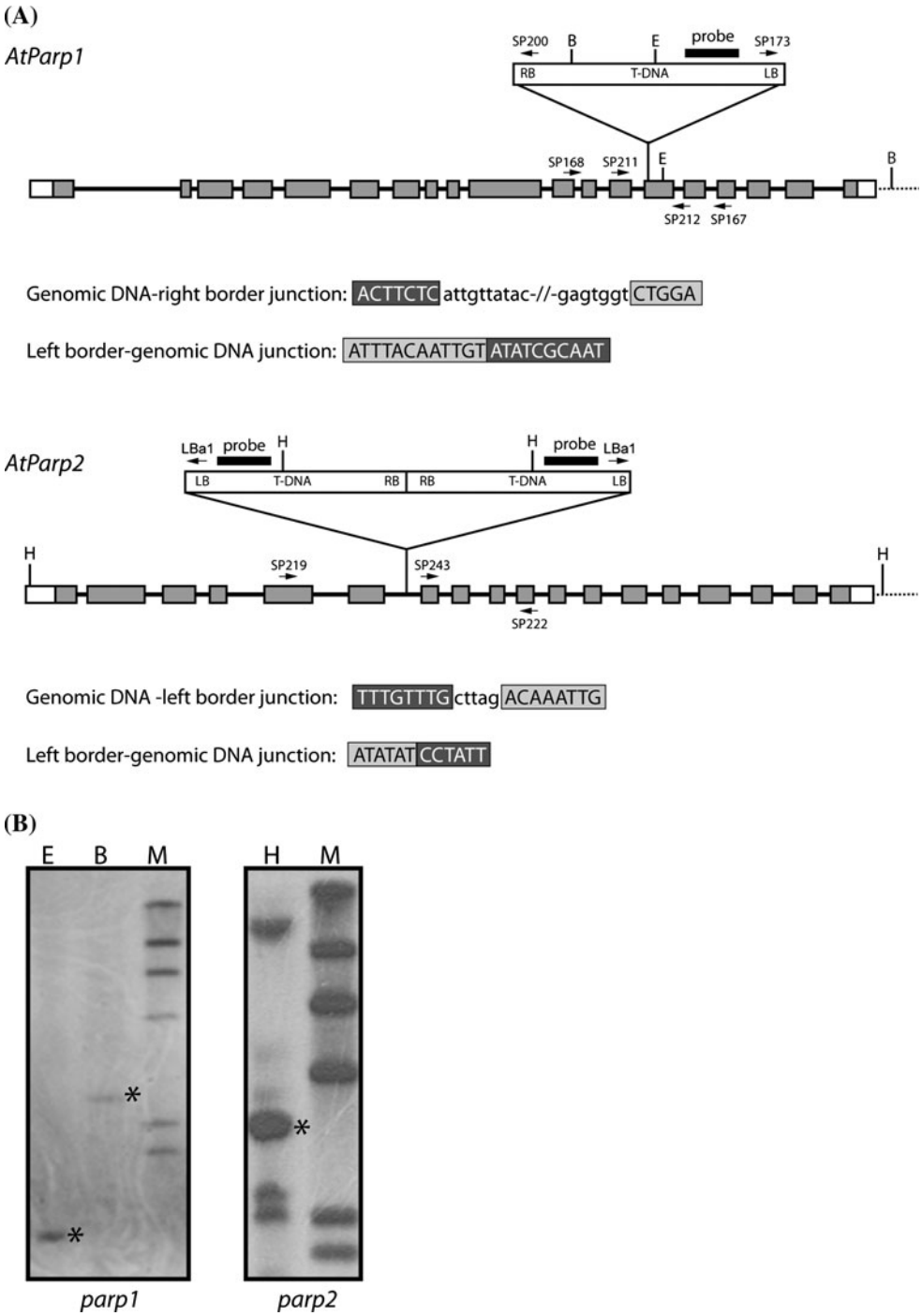

Fig. 1 Molecular analysis of the T-DNA insertion lines. **a** Genomic organization of the *PARP1* and *PARP2 loci* in the *parp1* and *parp2* mutants. Inserted T-DNAs of pGABI (*parp1*) or pROK2 (*parp2*) are indicated. Exons are shown as *grey boxes*, 3′ and 5′ UTRs are shown as *white boxes* and introns are shown as *lines*. The primers used for genotyping and Q-RT-PCR analysis are indicated. The probe and the restriction enzyme digestion sites (B for *Bgl*II; E for *Eco*RV; H for *Hin*dIII) used for Southern blot analysis are also indicated. The sequence of the T-DNA-genomic DNA junctions are shown: genomic DNA in *dark grey boxes*, T-DNA insertions in *light grey boxes* and filler DNA not boxed. **b** Southern blot analysis of the *parp1* and *parp2* mutants. DNA was digested with *Eco*RV, *Bgl*II or *Hin*dIII and separated on a 0.7 % agarose gel along a DIG-labeled Lambda *Eco*RI/*Hin*dIII marker (lane M), blotted and hybridized with a DIG-labeled T-DNA probe. The bands with the expected size are indicated with an *asterisk*

different pathways are impaired in the *p1p2* and *ku80* mutants.

In order to further quantify the DNA damage and repair in the mutants after MMS treatment, comet assays (A/N protocol) were performed to identify SSBs and DSBs. For each treatment, around 100 randomly chosen nuclei from 4 independent mini gel replicas were analyzed by using CometScore^{Tm}. Without any treatment *parp1*, *p1p2, p1p2k80* and *ku80* genomic DNA contained more damage than that of the wild type, demonstrating that PARP proteins and KU80 are involved in DNA repair (Fig. 3a). MMS treatment (0.01 %) for 2 h significantly increased the DNA damage in the *parp1*, *p1p2* and *p1p2k80* mutants, but not in the *parp2* and *ku80* mutants and the wild type (Fig. 3b). The *p1p2k80* triple mutant had significantly more DNA damage than the *p1p2* and the *ku80* mutant, in accordance with the result of the fresh weight measurements after the 0.008 % MMS treatment (Fig. 2b). MMS

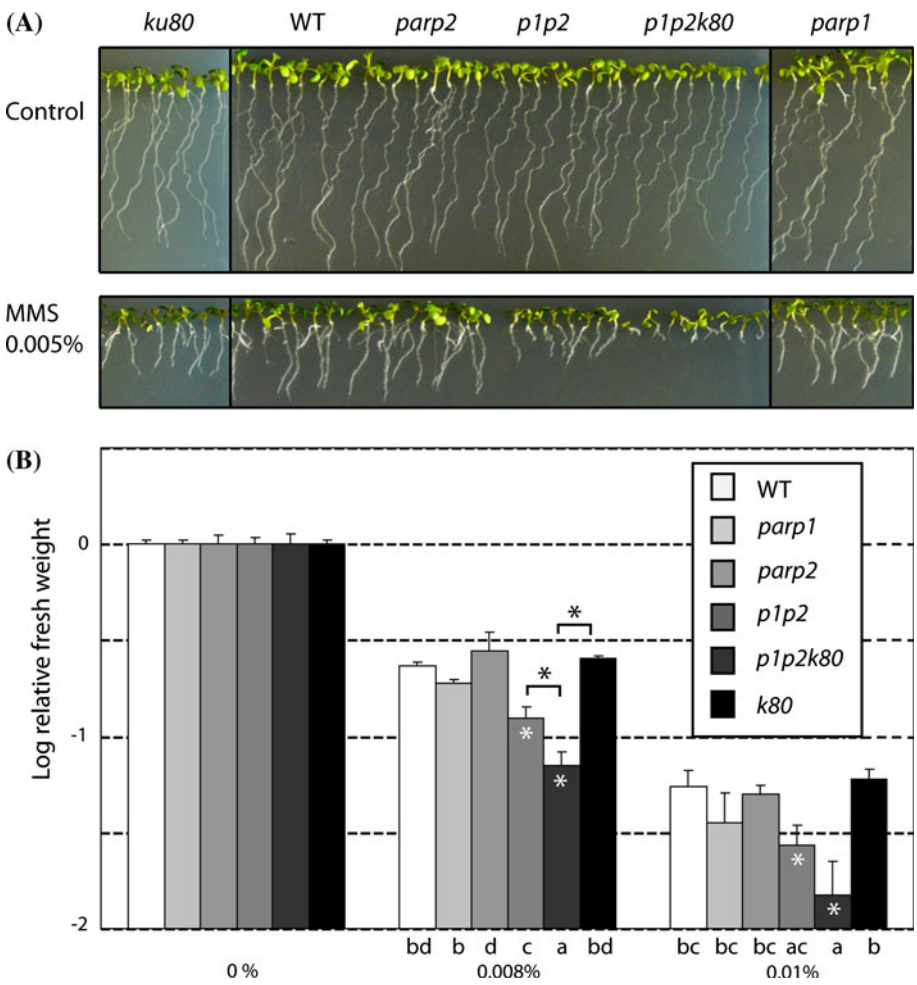

Fig. 2 Hypersensitivity of wild-type plants and *parp1*, *parp2*, *p1p2*, *p1p2k80 and ku80* mutants to DNA-damaging treatments. **a** Phenotypes of wild-type (WT) plants and mutants grown for two weeks on vertically positioned ½ MS plates (control) or plates containing 0.005 % MMS. **b** Fresh weight of 2-week-old wild-type plants (*white*) and *parp1* (*light grey*), *parp2* (*grey*), *p1p2* (*dark grey*), *p1p2k80* (*grey-black*) and *ku80* (*black*) mutants treated with 0, 0.008 % MMS or 0.01 % MMS. For each treatment 20 seedlings were weighed in triplicate. Fresh weight of the plants grown for 2 weeks without MMS was set at 1. Log values of the relative fresh weights are shown. Significant differences ($P < 0.05$) between the WT and mutants after the same treatment are indicated by asterisks within the bars and between selected mutant lines above the bars. Different groups are indicated by letters

treatment during 24 h was very deleterious to all plant lines and after 24 h of recovery more than half of the DNA damage was repaired compared to the situation before treatment.

In vitro end joining

In order to investigate whether PARP is involved in B-NHEJ in plants end-joining assays were performed in cell-free protein extracts from leaves with linear DNA substrates with different types of DNA ends (Table 1). Such method was used previously for biochemical characterization of factors involved in end joining in mammalian cell extracts, but so far not for plants. Since B-NHEJ often uses microhomology for end joining (MMEJ), the spectra of end joining products should reveal whether PARP is involved in MMEJ in plants. For comparison extracts of the wild type and the *ku80*, *p1p2* and *p1p2k80* mutants were used.

Analysis of the products by sequencing showed that end joining was accurate for the DNA substrates with compatible 5′-overhangs at the ends, whereas end joining was prone to be inaccurate for the other types of ends, such as compatible 3′-overhangs, incompatible ends and blunt ends (Tables 2, 3). In most cases inaccurate end joining resulted in deletions, suggesting DNA end resection took place before ligation. Small deletions (<10 bp) were often seen among the products from all the different plant lines. Large deletions (>10 bp) were rarely obtained for the wild type and the *p1p2* mutant. The number of large deletions was significantly higher in the *ku80* and *p1p2k80* mutants. This suggested that KU80 protected the DNA ends from resection and prevented the formation of large deletions. In the *ku80* mutant the ends were more often repaired by MMEJ. One large deletion (291 bp) found in the *ku80* mutant resulted from repair on regions of 8 bp microhomology.

In order to test whether PARP proteins are involved in MMEJ, a DNA substrate with blunt ends containing 10 bp microhomology sequences was used in end-joining assays. When end joining occurs via MMEJ using the 10 bp microhomology, an *Xcm*I site (CCAN9TGG) will be generated (Fig. 4). Analysis of the products showed that

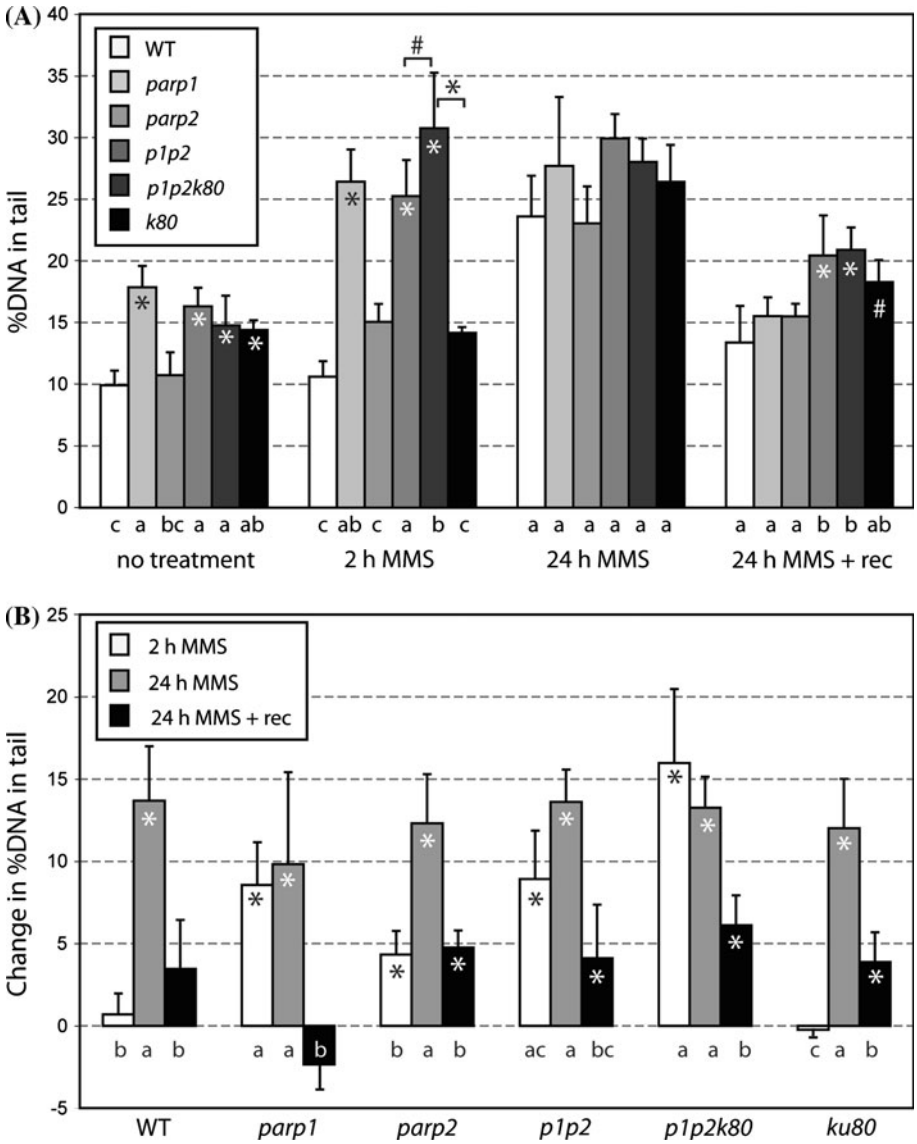

Fig. 3 Comet assay. **a** The fraction of DNA in comet tails (%DNA in tail) was used as a measure of DNA damage in wild-type plants (*white*) and *parp1* (*light grey*), *parp2* (*grey*), *p1p2* (*dark grey*), *p1p2k80* (*grey-black*) and *ku80* (*black*) mutants, without treatment or with 2 h MMS treatment (0.01 %), 24 h MMS treatment and 24 h MMS treatment followed by 24 h recovery. Significant differences between the wild type (WT) and mutants after the same treatment are indicated by asterisks ($P < 0.05$) or hashtags ($P < 0.1$) within the *bars* or between selected mutant lines above the *bars*. Different groups are indicated by letters. **b** Changes in %DNA in tail after treatment with MMS for 2 h (*white box*), 24 h (*grey box*) or 24 h followed by 24 h recovery (*black box*) compared to untreated plants. Significant differences compared to untreated plants are indicated by asterisks ($P < 0.05$). Different groups are indicated by *letters*

significantly less MMEJ products were obtained with the *p1p2* and *p1p2k80* extracts (Table 2). To further determine the fraction of the products joined via MMEJ using the 10 bp microhomology, the end joining products produced with wild type, *ku70*, *ku80*, *p1p2* or *p1p2k80* protein extracts were digested with *Xcm*I and analyzed by gel electrophoresis (Fig. 4). Compared with the wild type, the *ku70* and *ku80* mutants had almost four-fold more MMEJ products, whereas the *p1p2* and *p1p2k80* mutants had two- to 20-fold less MMEJ products, indicating that the PARP proteins are involved in MMEJ, while the KU proteins prevent MMEJ by the PARP proteins. This suggested that there is a competition between PARP and KU proteins to regulate the use of different NHEJ pathways. The products that were not repaired via MMEJ were sequenced and these were precisely joined blunt ends or contained small deletions or insertions (Table 2 and Table 3).

Discussion

Here *parp1*, *parp2*, *p1p2*, and *p1p2ku80* mutants were functionally characterized. The results from in vitro end-joining assays showed that also in plants PARPs are involved in a back-up pathway of DNA end joining. The *p1p2k80* mutant was clearly more sensitive to DNA damage than the *p1p2* and *ku80* mutants, indicating that different DNA repair pathways had been inactivated by the mutations. Nevertheless, the *p1p2k80* mutant could still repair DSBs according to the in vitro end joining assays, suggesting that either there is still another alternative NHEJ pathway in plants or that the C-NHEJ and B-NHEJ were not completely inactive. Possibly another PARP-like homologue plays a role in DNA repair in Arabidopsis, like PARP3, which was found to be involved in DNA damage repair in mammalian cells (Boehler et al. 2011).

Table 3 Sequences of junctions after in vitro end joining that were not sensitive for the restriction enzymes used (see Table 2)

5' overhangs (BamHI)	
	CAAGCTACCATCCTCAGC**G^GATCC**GAATTCGTAATCATGGTCATAGC
WT	CAAGCTACCATCCTCAGC··**ATCC**GAATTCGTAATCATGGTCATAGC
	CAAGCTACCATCCTCAG···**ATCC**GAATTCGTAATCATGGTCATAGC
3' overhangs (KpnI)	
	CAAGCTACCATCCTACAGC**GGTAC^C**GAATTCGTAATCATGGTCATAGC
WT	CAAGCTACCATCCTACAGC**GGTAC**·GAATTCGTAATCATGGTCATAGC (2)
	CAAGCTACCATCCTACAGC**GGT**···-145bp···ACTGCCCGCTTTCCA
p1p2	CAAGCTACCATCCTACAGC**GGTAC**·GAATTCGTAATCATGGTCATAGC
	CAAGCTACCATCCTACAGC**GGTACA**GAATTCGTAATCATGGTCATAGC
	CAAGCTACCATCCTACAGC**GGTACAACC**GAATTCGTAATCATGGTCATAG
	CAAGCTACCATCCTACAGC**GGTACGTACC**GAATTCGTAATCATGGTCATAG (2)
p1p2k80	CAAGCTACCATCCTACAGC**GGTAC**·GAATTCGTAATCATGGTCATAGC (2)
	CAAGCTACCATCCTACAGC**GGTACGTACC**GAATTCGTAATCATGGTCATAG (2)
ku80	CAAGCTACCATCCTACAGC**GGTAC**·GAATTCGTAATCATGGTCATAGC
	CAAGCTACCATCCTACAGC**GGTACGC**GAATTCGTAATCATGGTCATAGC
	CAAGCTACCATCCTACAGC**GGTACGTACC**GAATTCGTAATCATGGTCATAG (2)
	AAAATACCGC··-336bp···**TACC**GAATTCGTAATCATGGTCATAGC
	TCGCTATTACGCCAGCTG·····-291bp·····CATTAATGAATCGGC
3' overhangs (KpnI) +5' overhangs (EcoRI)	
	CAAGCTACCATCCTACAGC**GGTAC^C G^AATTC**GTAATCATGGTCATAGC
	CAAGCTACCATCCTACAGC**GGTACAATTC**GTAATCATGGTCATAGC
WT	CAAGCTACCATCCTACAGC**GGTA·AATTC**GTAATCATGGTCATAGC (2)
	CAAGCTACCATCCTACAGC**GGTAC·ATTC**GTAATCATGGTCATAGC (3)
	CAAGCTACCATCCTACAGC**GGTA··ATTC**GTAATCATGGTCATAGC
	CAAGCTACCATCCTACAGC**GGTAC···TC**GTAATCATGGTCATAGC
	CAAGCTACCATCCTACAGC**GGTAC····C**GTAATCATGGTCATAGC
	CAAGCTACCATCCTACAGC**GGTAC**·····GTAATCATGGTCATAGC (2)
	CAAGCTACCATCCTACAGC**G**·········GTAATCATGGTCATAGC
p1p2	CAAGCTACCATCCTACAGC**GGTA·AATTC**GTAATCATGGTCATAGC (2)
	CAAGCTACCATCCTACAGC**GGTAC·ATTC**GTAATCATGGTCATAGC
	CAAGCTACCATCCTACAGC**GGTAC**·····GTAATCATGGTCATAGC (2)
	CAAGCTACCATCCTACAGC**GGTA**·····GTAATCATGGTCATAGC
	CAAGCTACCATCCTACAGC**G**···-75bp···GCTCACAATTCCACA
p1p2k80	CAAGCTACCATCCTACAGC**GGTA·AATTC**GTAATCATGGTCATAGC
	CAAGCTACCATCCTACAGC**GGTAC·ATTC**GTAATCATGGTCATAGC (3)
	CAAGCTACCATCCTACAGC**GGTAC··TTC**GTAATCATGGTCATAGC
	CAAGCTACCATCCTACAGC**GGTAC···TC**GTAATCATGGTCATAGC
	CAAGCTACCATCCTACAGC**GGTAC····C**GTAATCATGGTCATAGC (3)
	CAAGCTACCATCCTACAGC**GGTAC**·····GTAATCATGGTCATAGC (4)
	CAAGCTACCATCCTACAGC**GGTAC**···-12bp···ATGGTCATAGC
	CAAGCTACCATCCTACAGC**GGTAC**····-14bp····GGTCATAGC
ku80	CAAGCTACCATCCTACAGC**GGTA·AATTC**GTAATCATGGTCATAGC
	CAAGCTACCATCCTACAGC**GGTAC**·····GTAATCATGGTCATAGC (4)
	CAAGCTACCATCCTACAGC**GGTA**·····GTAATCATGGTCATAGC (3)
	CAAGCTACCATCCTACAGC**GGTA**·····AATCATGGTCATAGC
	CAAGCTACCATCCTACAGC**GGTAC**····-14bp····GGTCATAGC
	CAAGCTACCATCCTACAGC**GGTAC**····-41bp·····TTATCCGC
	CAAGCTACCATCCTACAGC**GGTAC**····-118bp·····TAATGAG
Blunt ends without microhomology	
	GTGCCAAGCTACCATCCTACAGCTGGAATTCGTAATCATGGTCATAGC
WT	GTGCCAAGCTACCATCCTACA····GAATTCGTAATCATGGTCATAGC
	GTGCCAAGCTACCATCCTAC·····GAATTCGTAATCATGGTCATAGC (2)
	GTGCCAAGCTACCATCCTACAG····AATTCGTAATCATGGTCATAGC
	GTGCCAAGCTACCATCC·····GAATTCGTAATCATGGTCATAGC
	GCCAGTGCCAAGCTACCATCCTA···-91bp···AGTGTAAAGCCTGG
	GCATCAGAGCAGATTG···-251bp···GAATTCGTAATCATGGTCAT
p1p2	GTGCCAAGCTACCATCCTACAG··GGAATTCGTAATCATGGTCATAGC (2)
	GTGCCAAGCTACCATCCTACAG···GAATTCGTAATCATGGTCATAGC
	GTGCCAAGCTACCATCCTACA···GGAATTCGTAATCATGGTCATAGC (4)
	GTGCCAAGCTACCATCCTAC····GGAATTCGTAATCATGGTCATAGC (2)
	GTGCCAAGCTACCATCCTA·····GAATTCGTAATCATGGTCATAGC
	GTGCCAAGCTACCATCCTACA·····ATTCGTAATCATGGTCATAGC
	GTGCCAAGCTACC··········GGAATTCGTAATCATGGTCATAGC
p1p2k80	GTGCCAAGCTACCATCCTACAG·TGGAATTCGTAATCATGGTCATAGC (1)
	GTGCCAAGCTACCATCCTACAGC··GAATTCGTAATCATGGTCATAGC (2)
	GTGCCAAGCTACCATCCTACAG···GAATTCGTAATCATGGTCATAGC
	GTGCCAAGCTACCATCCTACAG····AATTCGTAATCATGGTCATAGC
	GTGCCAAGCTACCATCCTACA····GAATTCGTAATCATGGTCATAGC (2)
	GTGCCAAGCTACCATCCT·····CATAGC
	GTGCCAAGCTACCATCCTA·····C
	GCCAAGCTACCATCCTACAGC····-78bp·····CCGGAAGCATAA
ku80	GTGCCAAGCTACCATCCTACAGC··GAATTCGTAATCATGGTCATAGC
	GTGCCAAGCTACCATCCTACAG··GGAATTCGTAATCATGGTCATAGC
	GTGCCAAGCTACCATCCTACAG···GAATTCGTAATCATGGTCATAGC
	GTGCCAAGCTACCATCCTACA···GGAATTCGTAATCATGGTCATAGC
	GTGCCAAGCTACCATCCTAC····GGAATTCGTAATCATGGTCATAGC
	GTGCCAAGCTACCATCCTAC·····GAATTCGTAATCATGGTCATAGC (2)
	GTGCCAAGCTACCATCCTAC·····AATTCGTAATCATGGTCATAGC
	GTGCCAAGCTACCATCC·····GAATTCGTAATCATGGTCATAGC
	GTGCCAAGCTACCATC·····ATGGTCATAGC
	CCAGTGCCAAGCTACCATCC···-56bp···GCTCACAATTCCACACA
	ACGCCAGGGTTTTCCCAGTC···-204bp···GGGAAACCTGTCGTGC

Table 3 continued

The recognition sequences for restriction enzymes are shown as bold letters. The number in brackets indicates multiple clones obtained for that sequence. The dots represent deletions and shaded letters represent insertions. The microhomologous sequences are underlined

Blunt ends with microhomology	
	GTGCCAAGCTACCATCCTACAGCATCCTACAGCTGGAATTCGTAATCA
WT	GTGCCAAGCTACCATCCTACAG•ATCCTACAGCTGGAATTCGTAATCA (5)
p1p2	GTGCCAAGCTACCATCCTACAG•ATCCTACAGCTGGAATTCGTAATCA (8)
	GTGCCAAGCTACCATCCTA••••ATCCTACAGCTGGAATTCGTAATCA (2)
	GTGCCAAGCTACCATCCTACAGCAATCCTACAGCTGGAATTCGTAATCA
	GTGCCAAGCTACCATCCTACAGCGGATCCTACAGCTGGAATTCGTAATCA
	GTGCCAAGCTACCATCCTACAGCGTGATCCTACAGCTGGAATTCGTAATC
p1p2k80	GTGCCAAGCTACCATCCTACAG•ATCCTACAGCTGGAATTCGTAATCA (5)
	GTGCCAAGCTACCATCCTAC•••ATCCTACAGCTGGAATTCGTAATCA
	GTGCCAAGCTACCATCCTA••••ATCCTACAGCTGGAATTCGTAATCA
	GTGCCAAGCTACCATCCTACAGCATCATCCTACAGCTGGAATTCGTAATCA
	GTGCCAAGCTACCATCCTACAGCTGGGAATCCTACAGCTGGAATTCGTAA
ku80	GTGCCAAGCTACCATCCTACAG•ATCCTACAGCTGGAATTCGTAATCA (2)
	GTGCCAAGCTACCATCCTA••••ATCCTACAGCTGGAATTCGTAATCATG

In vitro end-joining assays were shown to be an easy and powerful tool for the biochemical characterization of factors involved in end joining in mammalian cells. We have applied such end-joining assay with plasmid DNA in cell-free extracts of Arabidopsis wild type and several mutants to assay for the effects of the mutations on the end-joining products. In our assays, deletions larger than 600 bp could not be identified due to the position of the PCR primers. It is therefore possible that we have missed some very large deletions, since it was reported earlier that they sometimes can reach up to 1.2 kb (Gorbunova and Levy 1997). In our assay we nevertheless clearly could identify the effects of the presence or absence of specific repair genes.

Analysis of DSB repair products *in planta* may reveal how DNA repair in various mutants is affected by the presence of chromatin. For such in vivo approach zinc finger nuclease-induced, meganuclease-induced and transposon-induced DSBs were shown to be useful tools (Pacher et al. 2007; Osakabe et al. 2010; Huefner et al. 2011; Lloyd et al. 2012). High-through put sequencing has made it possible to analyze many repair events in vivo. However, the use of these nucleases in vivo has the disadvantage that the variety of DNA ends is very limited.

Though NHEJ is an error-prone DNA repair pathway compared with HR, it still results in a high fidelity when KU-dependent C-NHEJ is active. Of the known end-joining pathways, C-NHEJ is relatively fast and accurate, so that it is the first choice for organisms to repair DNA DSBs. A relatively high percentage of end- joining products in assays with mammalian cells or extracts showed exact repair (Kuhfittig-Kulle et al. 2007; Mansour et al. 2010). Repair of nuclease-induced DSBs in plants containing 5′-overhangs also resulted in a high percentage of exactly repaired products (Lloyd et al. 2012). In our experiments we also found that the majority of the end-joining products of substrates with 5′-overhangs were accurate without deletions or insertions. Substrates with 3′-overhangs resulted in less accurately joined products compared to 5′-overhangs. Slower repair of the 3′-overhangs might be the cause of this observation, since it has been found that repair

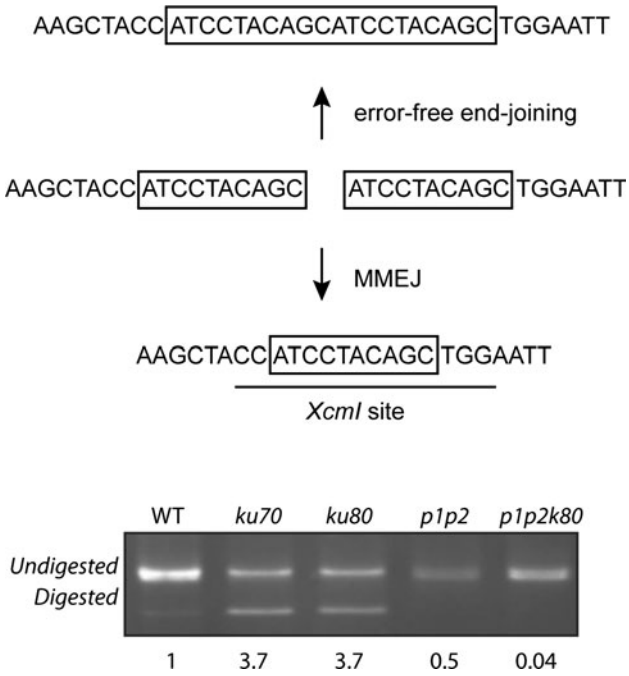

Fig. 4 Microhomology mediated end joining. Linear plasmid containing 10 bp homology at the ends (*boxed*) was used for in vitro end joining. The ends are either error-free joined via NHEJ or via MMEJ creating an *Xcm*I site. PCR products after end joining with protein extracts from wild-type plants, *ku70*, *ku80*, *p1p2* or *p1p2k80* mutants were digested with *Xcm*I to determine the fraction (relative to the wild type) that was joined via MMEJ (shown below the lanes)

of substrates with 3′-overhangs in mammalian extracts is slower than repair of substrates with 5′overhangs (Audebert et al. 2004).

The end-joining assays also revealed that more large deletions were formed in extracts from the *ku80* mutant than from the wild type, corroborating that KU80 plays a role in maintaining genome integrity in plants. Longer deletions were also found in KU80 deficient mammalian cells (Mansour et al. 2010). Repair of DSBs in the *p1p2* and *p1p2k80* mutants gave less MMEJ products than the wild type (Fig. 4; Table 3), indicating that PARP1 and PARP2 are involved in MMEJ. Repair of ZFN-induced

DSBs in another Arabidopsis *ku80* mutant also resulted in larger deletions as a consequence of MMEJ (Osakabe et al. 2010). Deep sequencing of repair products of transposon-induced DSBs also showed less accurate repair and revealed a shift towards MMEJ in NHEJ mutants (Huefner et al. 2011). This is in accordance with some reports in mammals, which showed that KU may serve as an alignment factor that not only increases NHEJ efficiency and accuracy, but also inhibits MMEJ (Feldmann et al. 2000; Chen et al. 2001; Kuhfittig-Kulle et al. 2007). These results point to a regulatory mechanism, in which competition between PARP and KU determines whether C-NHEJ or B-NHEJ is used (Wang et al. 2006). When the KU protein is absent, PARP may bind the DNA ends and direct the DNA repair pathway to B-NHEJ, which more often uses microhomology. Katsura et al. (2007) reported that KU80 is involved in MMEJ, but this is in contrast to our observations, since we showed that MMEJ occurred more frequently in the *ku80* mutant. Recently, it was shown that KU controls the choice of repair pathway by inhibiting end processing and thus repressing HR and MMEJ (Robert et al. 2009; Fattah et al. 2010). MMEJ leads to deletion and is therefore mutagenic and may be harmful for genome stability. When the major DNA DSB repair pathway, C-NHEJ is available, MMEJ is suppressed by C-NHEJ for optimal genome stability. The *p1p2k80* mutant may be used to identify components of the still unknown NHEJ pathways in future.

Acknowledgments We thank Dr. Li Liang for providing the plasmid PUC19PD1/4. This work was financially supported by the Chinese Scholarship Council (CSC) (QJ, HS) and the European Union Program EU Recbreed (KBBE-2008-227190) (SdP).

References

Ahmad A, Robinson AR, Duensing A, van Drunen E, Beverloo HB, Weisberg DB, Hasty P, Hoeijmakers JHJ, Niedernhofer LJ (2008) ERCC1-XPF endonuclease facilitates DNA double-strand break repair. Mol Cell Biol 28:5082–5092

Alonso J, Stepanova A, Leisse T, Kim C (2003) Genome-wide insertional mutagenesis of *Arabidopsis thaliana*. Science 301:653–657

Amé J-C, Rolli V, Schreiber V, Niedergang C, Apiou F, Decker P, Muller S, Höger T, Ménissier-de Murcia J, de Murcia G (1999) PARP-2, a novel mammalian DNA damage-dependent poly (ADP-ribose) polymerase. J Biol Chem 274:17860–17868

Amé J-C, Spenlehauer C, de Murcia G (2004) The PARP superfamily. BioEssays 26:882–893

Amor Y, Babiychuk E, Inze D, Levine A (1998) The involvement of poly(ADP-ribose) polymerase in the oxidative stress responses in plants. FEBS Lett 440:1–7

Audebert M, Salles B, Calsou P (2004) Involvement of poly(ADP-ribose) polymerase-1 and XRCC1/DNA ligase III in an alternative route for DNA double-strand breaks rejoining. J Biol Chem 279:55117–55126

Babiychuk E, Cottrill PB, Storozhenko S, Fuangthong M, Chen Y, O'Farrell MK, Van Montagu M, Inzé D, Kushnir S (1998) Higher plants possess two structurally different poly(ADP-ribose) polymerases. Plant J 15:635–645

Boehler C, Gauthier LR, Mortusewicz O, Biard DS, Saliou J-M, Bresson A, Sanglier-Cianferani S, Smith S, Schreiber V, Boussin F, Dantzer F (2011) Poly(ADP-ribose) polymerase 3 (PARP3), a newcomer in cellular response to DNA damage and mitotic progression. Proc Natl Acad Sci USA 108:2783–2788

Bryant HE, Petermann E, Schultz N, Jemth A-S, Loseva O, Issaeva N, Johansson F, Fernandez S, McGlynn P, Helleday T (2009) PARP is activated at stalled forks to mediate Mre11-dependent replication restart and recombination. EMBO J 28:2601–2615

Bundock P, van Attikum H, Hooykaas P (2002) Increased telomere length and hypersensitivity to DNA damaging agents in an *Arabidopsis KU70* mutant. Nucleic Acids Res 30:3395–3400

Caldecott KW (2003) XRCC1 and DNA strand break repair. DNA Repair 2:955–969

Charbonnel C, Gallego ME, White CI (2010) Xrcc1-dependent and Ku-dependent DNA double-strand break repair kinetics in Arabidopsis plants. Plant J 64:280–290

Charbonnel C, Allain E, Gallego ME, White CI (2011) Kinetic analysis of DNA double-strand break repair pathways in Arabidopsis. DNA Repair 10:611–619

Chen Y-M, Shall S, O'Farrell M (1994) Poly(ADP-ribose) polymerase in plant nuclei. Eur J Biochem 224:135–142

Chen S, Inamdar KV, Pfeiffer P, Feldmann E, Hannah MF, Yu Y, Lee JW, Zhou T, Lees-Miller SP, Povirk LF (2001) Accurate in vitro end joining of a DNA double strand break with partially cohesive 3′-overhangs and 3′-phosphoglycolate termini: effect of Ku on repair fidelity. J Biol Chem 276:24323–24330

Cheng Q, Barboule N, Frit P, Gomez D, Bombarde O, Couderc B, Ren G-S, Salles B, Calsou P (2011) Ku counteracts mobilization of PARP1 and MRN in chromatin damaged with DNA double-strand breaks. Nucleic Acids Res 39:9605–9619

De Block M, Verduyn C, De Brouwer D, Cornelissen M (2005) Poly(ADP-ribose) polymerase in plants affects energy homeostasis, cell death and stress tolerance. Plant J 41:95–106

de Pater S, Caspers M, Kottenhagen M, Meima H, ter Stege R, de Vetten N (2006) Manipulation of starch granule size distribution in potato tubers by modulation of plastid division. Plant Biotech J 4:123–134

Dibiase SJ, Zeng Z-C, Chen R, Hyslop T, Curran WJ, Iliakis G (2000) DNA-dependent protein kinase stimulates an independently active, nonhomologous, end-joining apparatus. Cancer Res 60:1245–1253

Fattah F, Lee EH, Weisensel N, Wang Y, Lichter N, Hendrickson EA (2010) Ku regulates the non-homologous end joining pathway choice of DNA double-strand break repair in human somatic cells. PLoS Genet 6:e1000855

Feldmann E, Schmiemann V, Goedecke W, Reichenberger S, Pfeiffer P (2000) DNA double-strand break repair in cell-free extracts from Ku80-deficient cells: implications for Ku serving as an alignment factor in non-homologous DNA end joining. Nucleic Acids Res 28:2585–2596

Fidantsef AL, Mitchell DL, Britt AB (2000) The Arabidopsis *UVH1* gene is a homolog of the yeast repair endonuclease *RAD1*. Plant Physiol 124:579–586

Friesner J, Britt AB (2003) *Ku80*- and *DNA ligase IV*-deficient plants are sensitive to ionizing radiation and defective in T-DNA integration. Plant J 34:427–440

Gallego ME, Bleuyard J-Y, Daoudal-Cotterell S, Jallut N, White CI (2003) Ku80 plays a role in non-homologous recombination but is not required for T-DNA integration in *Arabidopsis*. Plant J 35:557–565

Gorbunova V, Levy AA (1997) Non-homologous DNA end joining in plant cells is associated with deletions and filler DNA insertions. Nucleic Acids Res 25:4650–4657

Haber JE (2008) Alternative endings. Proc Natl Acad Sci USA 105:405–406

Heacock M, Spangler E, Riha K, Puizina J, Shippen DE (2004) Molecular analysis of telomere fusions in *Arabidopsis*: multiple pathways for chromosome end-joining. EMBO J 23:2304–2313

Hiom K (2010) Coping with DNA double strand breaks. DNA Repair 9:1256–1263

Huefner ND, Mizuno Y, Weil CF, Korf I, Britt AB (2011) Breadth by depth: expanding our understanding of the repair of transposon-induced DNA double strand breaks via deep-sequencing. DNA Repair 10:1023–1033

Iliakis G (2009) Backup pathways of NHEJ in cells of higher eukaryotes: cell cycle dependence. Radiother Onc 92:310–315

Jia Q, Bundock P, Hooykaas PJJ, de Pater S (2012) *Agrobacterium tumefaciens* T-DNA integration and gene-targeting in *Arabidopsis thaliana* non-homologous end-joining mutants. J Bot. doi: 10.1155/2012/989272

Katsura Y, Sasaki S, Sato M, Yamaoka K, Suzukawa K, Nagasawa T, Yokota J, Kohno T (2007) Involvement of Ku80 in microhomology-mediated end joining for DNA double-strand breaks in vivo. DNA Repair 6:639–648

Kuhfittig-Kulle S, Feldmann E, Odersky A, Kuliczkowska A, Goedecke W, Eggert A, Pfeiffer P (2007) The mutagenic potential of non-homologous end joining in the absence of the NHEJ core factors Ku70/80, DNA-PKcs and XRCC4-LigIV. Mutagenesis 22:217–233

Lepiniec L, Babiychuk E, Kushnir S, Van Montagu M, Inze M (1995) Characterization of an Arabidopsis thaliana cDNA homologue to animal poly(ADP-ribose) polymerase. FEBS Lett 364:103–108

Li J, Vaidya M, White C, Vainstein A, Citovsky V, Tzfira T (2005) Involvement of KU80 in T-DNA integration in plant cells. Proc Natl Acad Sci USA 102:19231–19236

Li Y, Rosso MG, Viehoever P, Weisshaar B (2007) GABI-Kat SimpleSearch: an Arabidopsis thaliana T-DNA mutant database with detailed information for confirmed insertions. Nucleic Acids Res 35:874–878

Liang L, Deng L, Nguyen SC, Zhao X, Maulion CD, Shao C, Tischfield JA (2008) Human DNA ligases I and III, but not ligase IV, are required for microhomology-mediated end joining of DNA double-strand breaks. Nucleic Acids Res 36:3297–3310

Lieber MR (2010) The mechanism of double-strand DNA break repair by the nonhomologous DNA end joining pathway. Ann Rev Biochem 3:181–211

Lloyd AH, Wang D, Timmis JN (2012) Single molecule PCR reveals similar patterns of non-homologous DSB repair in tobacco and arabidopsis. PLoS ONE 7:e32255

Mansour WY, Rhein T, Dahm-Daphi J (2010) The alternative end-joining pathway for repair of DNA double-strand breaks requires PARP1 but is not dependent upon microhomologies. Nucleic Acids Res 38:6065–6077

Masaoka A, Horton JK, Beard WA, Wilson SH (2009) DNA polymerase β and PARP activities in base excision repair in living cells. DNA Repair 8:1290–1299

McVey M, Lee SE (2008) MMEJ repair of double-strand breaks (director's cut): deleted sequences and alternative endings. Trends Genet 24:529–538

Menke M, Chen I-P, Angelis K, Schubert I (2001) DNA damage and repair in Arabidopsis thaliana as measured by the comet assay after treatment with different classes of genotoxins. Mut Res 493:87–93

Mladenov E, Iliakis G (2011) Induction and repair of DNA double strand breaks: the increasing spectrum of non-homologous end joining pathways. Mut Res 711:61–72

Nussenzweig A, Nussenzweig MC (2007) A backup DNA repair pathway moves to the forefront. Cell 131:223–225

O'Connor PJ (1981) Interaction of chemical carcinogens with macromolecules. J Cancer Res Clinical Onc 99:167–186

Osakabe K, Osakabe Y, Toki S (2010) Site-directed mutagenesis in *Arabidopsis* using custom-designed zinc finger nucleases. Proc Natl Acad Sci USA 107:12034–12039

Pacher M, Schmidt-Puchta W, Puchta H (2007) Two unlinked double-strand breaks can induce reciprocal exchanges in plant genomes via homologous recombination and nonhomologous end joining. Genetics 175:21–29

Puizina J, Siroky J, Mokros P, Schweizer D, Riha K (2004) Mre11 deficiency in arabidopsis is associated with chromosomal instability in somatic cells and Spo11-dependent genome fragmentation during meiosis. Plant Cell 16:1968–1978

Riha K, Watson JM, Parkey J, Shippen DE (2002) Telomere length deregulation and enhanced sensitivity to genotoxic stress in *Arabidopsis* mutants deficient in Ku70. EMBO J 21:2819–2826

Robert I, Dantzer F, Reina-San-Martin B (2009) Parp1 facilitates alternative NHEJ, whereas Parp2 suppresses IgH/c-myc translocations during immunoglobulin class switch recombination. J Exp Med 206:1047–1056

Rosidi B, Wang M, Wu W, Sharma A, Wang H, Iliakis G (2008) Histone H1 functions as a stimulatory factor in backup pathways of NHEJ. Nucleic Acids Res 36:1610–1623

San Filippo J, Sung P, Klein H (2008) Mechanism of eukaryotic homologous recombination. Ann Rev Biochem 77:229–257

Schreiber V, Amé J-C, Dollé P, Schultz I, Rinaldi B, Fraulob V, Ménissier-de Murcia J, de Murcia G (2002) Poly(ADP-ribose) polymerase-2 (PARP-2) is required for efficient base excision DNA repair in association with PARP-1 and XRCC1. J Biol Chem 277:23028–23036

Schreiber V, Dantzer F, Ame J-C, de Murcia G (2006) Poly(ADP-ribose): novel functions for an old molecule. Nature Rev Mol Cell Biol 7:517–528

Shrivastav M, De Haro LP, Nickoloff JA (2008) Regulation of DNA double-strand break repair pathway choice. Cell Res 18:134–147

Tamura K, Adachi Y, Chiba K, Oguchi K, Takahashi H (2002) Identification of Ku70 and Ku80 homologues in *Arabidopsis thaliana*: evidence for a role in the repair of DNA double- strand breaks. Plant J 29:771–781

Uchiyama Y, Suzuki Y, Sakaguchi K (2008) Characterization of plant XRCC1 and its interaction with proliferating cell nuclear antigen. Planta 227:1233–1241

van Attikum H, Bundock P, Overmeer RM, Lee L-Y, Gelvin SB, Hooykaas PJJ (2003) The Arabidopsis *AtLIG4* gene is required for the repair of DNA damage, but not for the integration of *Agrobacterium* T-DNA. Nucleic Acids Res 31:4247–4255

Vanderauwera S, De Block M, Van de Steene N, van de Cotte B, Metzlaff M, Van Breusegem F (2007) Silencing of poly(ADP-ribose) polymerase in plants alters abiotic stress signal transduction. Proc Natl Acad Sci USA 104:15150–15155

Wang H, Perrault AR, Takeda Y, Qin W, Wang H, Iliakis G (2003) Biochemical evidence for Ku-independent backup pathways of NHEJ. Nucleic Acids Res 31:5377–5388

Wang M, Wu W, Wu W, Rosidi B, Zhang L, Wang H, Iliakis G (2006) PARP-1 and Ku compete for repair of DNA double strand breaks by distinct NHEJ pathways. Nucleic Acids Res 34:6170–6182

West CE, Waterworth WM, Jiang Q, Bray CM (2000) *Arabidopsis* DNA ligase IV is induced by γ-irradiation and interacts with an *Arabidopsis* homologue of the double strand break repair protein XRCC4. Plant J 24:67–78

West CE, Waterworth WM, Story GW, Sunderland PA, Jiang Q, Bray CM (2002) Disruption of the *Arabidopsis AtKu80* gene demonstrates an essential role for AtKu80 protein in efficient repair of DNA double-strand breaks in vivo. Plant J 31:517–528

Woodhouse BC, Dianov GL (2008) Poly ADP-ribose polymerase-1: an international molecule of mystery. DNA Repair 7:1077–1086

Woodhouse BC, Dianova II, Parsons JL, Dianov G (2008) Poly(ADP-ribose) polymerase-1 modulates DNA repair capacity and prevents formation of DNA double strand breaks. DNA Repair 7:932–940

Wu W, Wang M, Wu W, Singh SK, Mussfeldt T, Iliakis G (2008) Repair of radiation induced DNA double strand breaks by backup NHEJ is enhanced in G2. DNA Repair 7:329–338

Xie A, Kwok A, Scully R (2009) Role of mammalian Mre11 in classical and alternative nonhomologous end joining. Nature Struct Mol Biol 16:814–818

Yélamos J, Schreiber V, Dantzer F (2008) Toward specific functions of poly(ADP-ribose) polymerase-2. Trends Mol Med 14:169–178